 CMES, vol.61, no.2, pp.177-200, 2010

Dynamic Analysis of Porous Media Considering Unequal Phase Discretization by Meshless Local Petrov-Galerkin Formulations

Delfim Soares Jr.[1]

Abstract: In this work, meshless methods based on the local Petrov-Galerkin approach are employed for the time-domain dynamic analysis of porous media. For the spatial discretization of the pore-dynamic model, MLPG formulations adopting Gaussian weight functions as test functions are considered, as well as the moving least square method is used to approximate the incognita fields. For time discretization, the generalized Newmark method is adopted. The present work is based on the **u**-p formulation and the incognita fields of the coupled analysis in focus are the solid skeleton displacements and the interstitial fluid pore pressures. Independent spatial discretization is considered for each phase of the model, rendering a more flexible, efficient and robust methodology. At the end of the paper, numerical applications illustrate the accuracy and potentialities of the proposed techniques.

Keywords: Meshless Local Petrov-Galerkin, Moving Least Squares, Time-Domain Analysis, Pore-Dynamics, Saturated Soils, Independent Phase Discretization.

1 Introduction

For many everyday engineering problems, such as earthquake engineering, soil-structure interaction, biomechanics, seismic wave scattering etc., dynamic porous media analysis is necessary and over simplified theoretical models (e.g., pure elastodynamic theory etc.) may only represent a very crude approximation. Nowadays, several numerical approaches, especially those considering finite element procedures, are available to analyse complex dynamic porous media (see, for instance, Ehlers and Bluhm, 1998; Lewis and Schrefler, 1998; Zienkiewicz *et al*., 1999; etc.) and most of these approaches are based on the pioneering work of Biot (Biot, 1941; 1956a-b; 1962 – for a complete overview of the porous media theory evolution, the book of de Boer, 1998, is recommended).

[1] Structural Engineering Department, Federal University of Juiz de Fora, Cidade Universitária, CEP 36036-330, Juiz de Fora, MG, Brazil. Tel: +55 32 2102-3468; E-mail: delfim.soares@ufjf.edu.br

In spite of the great success of the finite element method as an effective numerical tool for the solution of boundary value problems on complex domains, there is still a growing interest in development of new advanced methods. Nowadays, many meshless formulations are becoming popular, due to their high adaptivity and to their low-cost effort to prepare input data (meshless methods were essentially stimulated by difficulties related to mesh generation). In addition, the need for flexibility in the selection of approximating functions (*e.g.*, the flexibility to use non-polynomial approximating functions) has played a significant role in the development of meshless methods (many meshless approximations give continuous variation of the first or higher order derivatives of a primitive function in counterpart to classical polynomial approximation where secondary fields have a jump on the interface of elements. Therefore, meshless approximations are leading to more accurate results in many cases).

A variety of meshless methods has been proposed along the last decade to analyse porous media. Mostly, these formulations have been applied to analyse consolidation problems and, presently, there are only some few works concerned with the dynamic analysis of porous media. Wang and co-authors (2002, 2004, 2005) present the numerical analysis of Biot's consolidation process, wave-induced transient response of seabeds and dissipation process of excess pore water pressure, respectively, by the radial point interpolation method (RPIM). Nogami *et al.* (2004) develop a numerical method for consolidation analysis of lumpy clay fillings by using the double porosity model and the RPIM, considering different order of interpolation functions. Wang *et al.* (2007) also present an unequal-order radial interpolation meshless method for Biot's consolidation theory. The consolidation analysis of saturated soils with anisotropic damage and the simulation of wave motions in saturated porous media are presented by Wang *et al.* (2008) and Chen and Li (2008), respectively, taking into account the RPIM. Considering the element-free Galerkin method (EFGM), Modaressi and Aubert (1998) are among the firsts studying deforming multiphase porous media. Murakami *et al.* (2005) describe a formulation for soil-water coupled problems considering finite strain analysis; Wang and Li (2006) and Wang *et al.* (2007) analyse factors influencing the solution of the consolidation problem and seabed instability, respectively; and Karim *et al.* (2002) study the transient response of saturated porous elastic soil under cyclic loading. Some numerical issues using element-free Galerkin meshless method for coupled hydro-mechanical problems are discussed by Oliaei *et al.* (2009). Meshless methods, based on the meshless local Petrov-Galerkin (MLPG) approach, are developed and implemented for the solution of the Biot's consolidation problem by Ferronato *et al.* (2007) and Bergamaschi (2009), taking into account axi-symmetric poroelastic models, and by Wang *et al.* (2009), taking into account plane models.

As far as the author is concerned, there are no publications regarding the dynamic analysis of porous media by MLPG formulations.

The present work is focused on the numerical modelling of saturated soils (i.e., soils that are composed of a solid phase with voids filled with water) and is based on the **u**-p formulation, as presented by Zienkiewicz and co-authors (1984, 1990). As commonly reported, the **u**-p formulation is a very attractive approach because of both its performance and simplicity. The variables of the model are, in this case, the displacements of the soil skeleton (**u**) and the pressures of the pore fluid (p). In this work, the solid and fluid sub-domains of the porous model are analysed considering complete independent discretizations by MLPG techniques. This means that, for each phase of the model, not only different order for the interpolation functions may be considered, but also complete disassociated node distributions (as well as test and weight functions, which is not explored in the present paper). This is highly important when impermeable and incompressible media are modelled, ensuring unique solvability and convergence of the analyses.

Considering finite element discretizations, in the limit of zero compressibility of water and soil grains and zero permeability, the functions used to interpolate displacements and pressures must fulfil either the Babuska-Brezzi (Babuska, 1973; Brezzi, 1974) conditions or the simpler patch test proposed by Zienkiewicz *et al*. (1986). These requirements exclude the use of elements with equal order interpolation for pressures and displacements, for which spurious oscillations may appear. Several works have been presented regarding this matter in a pore-dynamic finite element context, as for instance, the work of Huang and Zienkiewicz (1998), which presents a new class of unconditionally stable staggered implicit-implicit time-stepping algorithms for coupled soil-pore fluid dynamic problems; Pastor *et al*. (1999), which describes a stabilization technique that allows the use of both linear triangles or both bilinear quadrilaterals for displacements and pressures; Pastor *et al*. (2000) and Li *et al*. (2003), proposing a generalization of the fractional-step method and its modified version, respectively; Soares (2008) describing an uncoupled time-marching technique that is based on implicit Green's functions; etc. (Huang *et al*., 2004, summarize the stabilization techniques that have been proposed in the literature to overcome volumetric locking for the incompressible or nearly incompressible soil dynamic behaviours).

The MLPG formulation considered here adopts Gaussian weight functions as test functions and employ the moving least square method to approximate the solid skeleton and the interstitial fluid incognita fields (for further details on related topics concerning MLPG formulations, the following references are indicated: Atluri and Zhu, 1998; Atluri and Shen, 2002; Lin and Atluri, 2000; Sladek *et al*., 2003, 2006; Soares *et al*., 2010 etc.). For time discretization, the generalized Newmark method

is adopted. At the end of the paper, numerical results are presented, illustrating the accuracy and potentialities of the proposed methodologies, taking into account the analysis of permeable and/or compressible media, as well as of impermeable and incompressible media.

2 Governing equations

The present work is focused on the $\mathbf{u}-p$ formulation, as presented by Zienkiewicz *et al*. (1984, 1990). In this case, the governing equations of the pore-dynamic model can be written as:

$$\sigma_{ij,j} - \rho_m \ddot{u}_i + \rho_m b_i = 0 \tag{1}$$

$$\alpha \dot{\varepsilon}_{ii} - (\kappa p_{,j})_{,i} + (1/Q)\dot{p} - a = 0 \tag{2}$$

where equation (1) stands for the balance of momentum of the mixture and equation (2) is a combination of the balance of mass and momentum for the interstitial fluid. In equation (1), $\sigma_{ij}(X,t)$ is the total Cauchy stress (usual indicial notation for Cartesian axes is considered); the effective stress is defined as $\sigma'_{ij} = \sigma_{ij} + \alpha \delta_{ij} p$, where $\alpha(X)$ accounts for slight strain changes, $p(X,t)$ stands for interstitial fluid pore-pressure and δ_{ij} represents the Kronecker delta ($\delta_{ij} = 0$ if $i \neq j$ and $\delta_{ij} = 1$ if $i = j$). Further on in equation (1), $u_i(X,t)$ stands for the solid matrix displacement and $b_i(X,t)$ for the body force distribution. Inferior commas and overdots indicate partial space ($u_{j,i} = \partial u_j / \partial x_i$) and time ($\dot{u}_i = \partial u_i / \partial t$) derivatives, respectively. $\rho_m = \upsilon \rho_f + (1-\upsilon)\rho_s$ stands for the mass density of the mixture, where $\rho_s(X)$ and $\rho_f(X)$ are the mass density of the solid and fluid phase, respectively, and $\upsilon(X)$ is the porosity of the medium. In equation (2), $\varepsilon_{ij}(X,t)$ represents the strain tensor and $\kappa(X)$ defines the permeability coefficients, according to the D'Arcy seepage law. $a(X,t)$ stands for domain source terms and the mixture parameter $Q(X)$ is defined by $(1/Q) = \mu/K_f + (\alpha - \mu)/K_s$, where the bulk moduli of the solid and fluid phase are represented by $K_s(X)$ and $K_f(X)$, respectively. In the present work, linear kinematical and constitutive relations are focused and they are represented by $\varepsilon_{ij} = \frac{1}{2}(u_{i,j} + u_{j,i})$ and $\sigma'_{ij} = D_{ijkl}\varepsilon_{kl} = \lambda \delta_{ij}\varepsilon_{kk} + 2\mu\, \varepsilon_{ij}$, respectively, where $D_{ijkl} = \lambda \delta_{ij}\delta_{kl} + \mu\,(\delta_{ik}\delta_{jl} + \delta_{il}\delta_{jk})$ is the elastic constitutive tensor and $\lambda(X)$ and $\mu(X)$ are the Lamé's constants of the medium. The boundary and initial conditions for the problem are given by:

(i) Boundary conditions ($t > 0, X \in \Gamma$ where $\Gamma = \Gamma_u \cup \Gamma_\tau = \Gamma_p \cup \Gamma_q$)

$$u_i(X,t) = \bar{u}_i(X,t) \text{ for } X \in \Gamma_u \tag{3a}$$

$$\tau_i(X,t) = \sigma_{ij}(X,t)\, n_j(X) = \bar{\tau}_i(X,t) \text{ for } X \in \Gamma_\tau \tag{3b}$$

$$p(X,t) = \bar{p}(X,t) \text{ for } X \in \Gamma_p \tag{3c}$$

$$q(X,t) = p_{,j}(X,t)\, n_j(X) = \bar{q}(X,t) \text{ for } X \in \Gamma_q \tag{3d}$$

(ii) Initial conditions ($t = 0$, $X \in \Gamma \cup \Omega$)

$$u_i(X,0) = \bar{u}_{i0}(X) \tag{4a}$$

$$\dot{u}_i(X,0) = \dot{\bar{u}}_{i0}(X) \tag{4b}$$

$$p_i(X,0) = \bar{p}_{i0}(X) \tag{4c}$$

where the prescribed values are indicated by over bars and $q(X,t)$ and $\tau_i(X,t)$ represent the fluxes and total tractions, respectively, acting along the boundary whose unit outward normal vector components are represented by $n_i(X)$. The effective tractions are defined as $\tau_i' = \tau_i + \alpha n_i p$. The domain of the model is denoted by Ω and the boundary by Γ ($\Gamma_u \cup \Gamma_\tau = \Gamma_p \cup \Gamma_q = \Gamma$ and $\Gamma_u \cap \Gamma_\tau = \Gamma_p \cap \Gamma_q = 0$).

3 Numerical discretization

In this section, the numerical discretization of the pore-dynamic model by a meshless local Petrov-Galerkin formulation is presented. First, in sub-section 3.1, the moving least square (MLS) approximation is described and, next (sub-section 3.2), the local weak-forms of the governing equations, as well as their spatial discretizations taking into account MLS approximations, are discussed. In sub-section 3.3, time-marching procedures based on the generalized Newmark method are presented, allowing the time-domain solution of the matricial systems of equations that arise.

3.1 Moving least square approximation

In general, a meshless method uses a local approximation to represent the trial function in terms of nodal unknowns which are either the nodal values of real field variables or fictitious nodal unknowns at some randomly located nodes. The moving least squares approximation may be considered as one of such schemes, and it is employed here.

Consider a sub-domain Ω_x, the neighbourhood of a point X and denoted as the domain of definition of the MLS approximation for the trial function at X, which is located in the problem domain Ω (see Fig.1). Also consider a generic field φ, which represents the interstitial fluid pore-pressure field p or the solid skeleton displacement field u_i. To approximate the distribution of function φ in Ω_x, over a

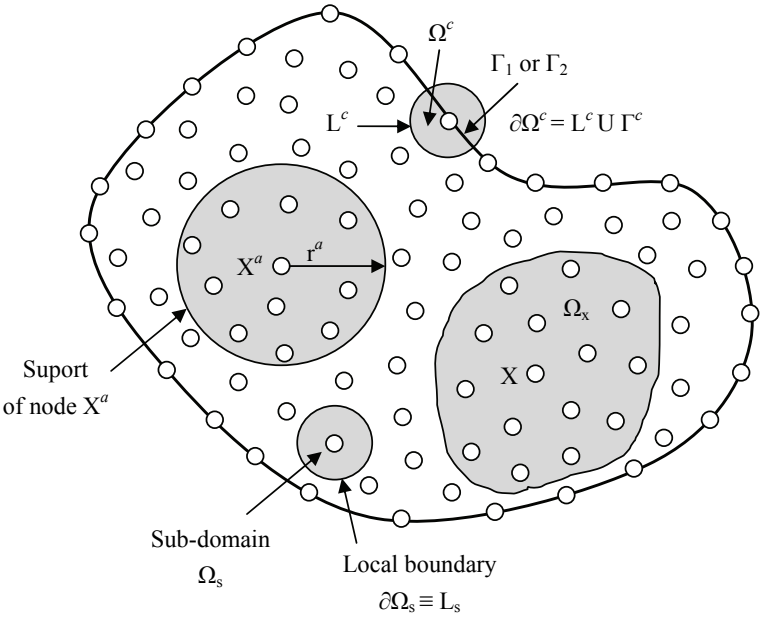

Figure 1: Local boundaries, sub-domains and domain of definition of the MLS approximation for the trial function at node X.

number of randomly located nodes, the MLS approximation of φ can be defined by (Atluri and Shen, 2002; Atluri, 2004):

$$\phi(X,t) \approx \mathbf{\Pi}^T(X)\hat{\Phi}(t) = \sum_{a=1}^{N} \eta^a(X)\hat{\phi}^a(t) \tag{5}$$

where $\hat{\phi}$ is the fictitious nodal value of ϕ and N is the number of points in the sub-domain Ω_x. The shape matrix $\mathbf{\Pi}^T(X) = \begin{bmatrix}\eta^1(X) & \eta^2(X) & \cdots & \eta^N(X)\end{bmatrix}$ is computed by:

$$\mathbf{\Pi}^T(X) = \mathbf{p}^T(X)\mathbf{A}^{-1}(X)\mathbf{B}(X) \tag{6}$$

where

$$\mathbf{A}(X) = \sum_{a=1}^{N} w^a(X)\mathbf{p}(X^a)\mathbf{p}^T(X^a) \tag{7a}$$

$$\mathbf{B}(X) = \begin{bmatrix} w^1(X)\mathbf{p}(X^1) & w^2(X)\mathbf{p}(X^2) & \cdots & w^N(X)\mathbf{p}(X^N)\end{bmatrix} \tag{7b}$$

and $\mathbf{p}^T(X) = \begin{bmatrix} p_1(X) & p_2(X) & \cdots & p_m(X) \end{bmatrix}$ is a complete monomial basis of order m. $w^a(X)$ is the weight function associated with node a. The Gaussian weight function is adopted here, and it is given by:

$$w^a(X) = \frac{\exp[-(d_a/c_a)^{2k}] - \exp[-(r_a/c_a)^{2k}]}{1 - \exp[-(r_a/c_a)^{2k}]}(1 - H[d_a - r_a]) \tag{8}$$

where $d_a = ||X - X^a||$ is the distance between the sampling point X and node X^a, c_a is a constant controlling the shape of the weight function and r_a is the radius of the circular support of the weight function. The Heaviside unit step function is defined as $H[z] = 1$ for $z > 0$ and $H[z] = 0$ for $z \leq 0$. The size of the weight function support should be large enough to have a sufficient number of nodes covered in the domain of definition to ensure the regularity of matrix $\mathbf{A}$.

3.2 Spatial discretization

Instead of writing the global weak-form for the governing equations described in section 2, the MLPG method constructs a weak-form over local fictitious sub-domains, such as Ω_s, which is a small region taken for each node inside the global domain (see Fig.1). The local sub-domains overlap each other, and cover the whole global domain Ω. The geometrical shape and size of local sub-domains can be arbitrary. In the present work, the local sub-domains are taken to be of circular shape. The local weak-form of the governing equations described in section 2 can be written as:

$$\int_{\partial\Omega_s} \varphi_{ik}\sigma_{ij}n_j\,d\Gamma - \int_{\Omega_s} \varphi_{ik,j}\sigma_{ij}\,d\Omega + \int_{\Omega_s} \varphi_{ik}(\rho_m b_i - \rho_m \ddot{u}_i)\,d\Omega + \beta \int_{\Gamma_{su}} \varphi_{ik}(u_i - \bar{u}_i)\,d\Gamma = 0 \tag{9a}$$

$$\int_{\partial\Omega_s} \varphi\,\kappa q\,d\Gamma - \int_{\Omega_s} \varphi_{,i}\,\kappa p_{,i} d\Omega + \int_{\Omega_s} \varphi\,(a - (1/Q)\dot{p} - \alpha\dot{\varepsilon}_{ii})\,d\Omega + \beta \int_{\Gamma_{sp}} \varphi\,(p - \bar{p})\,d\Gamma = 0 \tag{9b}$$

where φ and φ_{ik} are test functions and β is a penalty parameter, which is introduced here in order to impose essential prescribed boundary conditions in an integral form. In equations (9), $\partial\Omega_s$ is the boundary of the local sub-domain, which consists of three parts, in general: $\partial\Omega_s = L_s \cup \Gamma_{s1} \cup \Gamma_{s2}$ (see Fig.1). Here, L_s is the local boundary that is totally inside the global domain, Γ_{s2} is the part of the local boundary which coincides with the global natural boundary, i.e., $\Gamma_{s2} = \partial\Omega_s \cap \Gamma_2$ (where Γ_2 stands for the natural boundary, i.e., $\Gamma_2 \equiv \Gamma_q$ or $\Gamma_2 \equiv \Gamma_\tau$) and, similarly,

Γ_{s1} is the part of the local boundary that coincides with the global essential boundary, i.e., $\Gamma_{s1} = \partial\Omega_s \cap \Gamma_1$ (where Γ_1 stands for the essential boundary, i.e., $\Gamma_1 \equiv \Gamma_p$ or $\Gamma_1 \equiv \Gamma_u$).

In this work, plane strain problems are focused and the variables of the solid skeleton are written considering the Voigt notation (i.e., $\sigma = \begin{bmatrix}\sigma_{11} & \sigma_{22} & \sigma_{12}\end{bmatrix}^T$, $\varepsilon = \begin{bmatrix}\varepsilon_{11} & \varepsilon_{22} & 2\varepsilon_{12}\end{bmatrix}^T$, $\tau = \begin{bmatrix}\tau_1 & \tau_2\end{bmatrix}^T$, $\mathbf{u} = \begin{bmatrix}u_1 & u_2\end{bmatrix}^T$ and $\mathbf{b} = \begin{bmatrix}b_1 & b_2\end{bmatrix}^T$). For plane strain models, the total and effective stresses can be expressed as:

$$\sigma = \sigma' - \mathbf{m}\alpha p = \begin{bmatrix}\sigma'_{11} & \sigma'_{22} & \sigma'_{12}\end{bmatrix}^T - \begin{bmatrix}1 & 1 & 0\end{bmatrix}^T \alpha p \tag{10a}$$

$$\sigma' = \mathbf{D}\varepsilon = \begin{bmatrix}\lambda+2\mu & \lambda & 0 \\ \lambda & \lambda+2\mu & 0 \\ 0 & 0 & \mu\end{bmatrix} \begin{bmatrix}\frac{\partial}{\partial x_1} & 0 \\ 0 & \frac{\partial}{\partial x_2} \\ \frac{\partial}{\partial x_2} & \frac{\partial}{\partial x_1}\end{bmatrix} \begin{bmatrix}u_1 \\ u_2\end{bmatrix} \tag{10b}$$

where $\mathbf{D}$ is the constitutive matrix and vector $\mathbf{m}$ plays the role of the Kronecker delta δ_{ij}.

Equations (9) can be rewritten taking into account expressions (5) and (10) and defining the local integral sub-domain as the circle Ω^c, centred at node X^c and described by radius r_c ($\partial\Omega^c = L^c \cup \Gamma_1^c \cup \Gamma_2^c$). The expressions that arise, considering the test functions as the Gaussian weight functions (i.e., $\varphi = w^c$ and $\varphi_{ik} = \delta_{ik} w^c$), which have vanishing values on L^c, are given by:

$$\begin{aligned}
&\sum_{a=1}^{N}\left(\int_{\Omega^c} w^c \rho_m \eta^a d\Omega\right)\ddot{\hat{\mathbf{u}}}^a + \\
&+\sum_{a=1}^{N}\left(\int_{\Omega^c}\mathbf{W}^c\mathbf{D}\mathbf{S}^a d\Omega - \int_{\Gamma_u^c} w^c \mathbf{N}\mathbf{D}\mathbf{S}^a d\Gamma - \beta\int_{\Gamma_u^c} w^c \eta^a d\Gamma\right)\hat{\mathbf{u}}^a + \\
&-\sum_{a=1}^{N}\left(\int_{\Omega^c}\mathbf{w}^c\alpha\eta^a d\Omega - \int_{\Gamma_u^c} w^c \mathbf{n}\alpha\eta^a d\Gamma\right)\hat{p}^a = \\
&=\int_{\Gamma_\tau^c} w^c \bar{\tau}\, d\Gamma + \int_{\Omega^c} w^c \rho_m \mathbf{b}\, d\Omega - \beta\int_{\Gamma_u^c} w^c \bar{\mathbf{u}} d\Gamma
\end{aligned} \tag{11a}$$

$$\sum_{a=1}^{N}\left(\int_{\Omega^c} w^c (1/Q)\,\eta^a d\Omega\right)\dot{\hat{p}}^a$$
$$+\sum_{a=1}^{N}\left(\int_{\Omega^c}\mathbf{w}^{cT}\boldsymbol{\kappa}\mathbf{s}^{aT}d\Omega-\int_{\Gamma_p^c} w^c\mathbf{n}^T\boldsymbol{\kappa}\mathbf{s}^{aT}d\Gamma-\beta\int_{\Gamma_p^c} w^c\eta^a d\Gamma\right)\hat{p}^a+ \tag{11b}$$
$$+\sum_{a=1}^{N}\left(\int_{\Omega^c} w^c\boldsymbol{\alpha}\mathbf{s}^a d\Omega\right)\dot{\hat{\mathbf{u}}}^a=\int_{\Gamma_q^c} w^c\boldsymbol{\kappa}\bar{q}\,d\Gamma+\int_{\Omega^c} w^c a\,d\Omega-\beta\int_{\Gamma_u^c} w^c\bar{p}d\Gamma$$

where matrices $\mathbf{N}$, $\mathbf{n}$, $\mathbf{W}^a$, $\mathbf{w}^a$, $\mathbf{S}^a$ and $\mathbf{s}^a$ are specified as:

$$\mathbf{N}=\begin{bmatrix} n_1 & 0 & n_2\\ 0 & n_2 & n_1\end{bmatrix} \tag{12a}$$

$$\mathbf{n}=\begin{bmatrix} n_1 & n_2\end{bmatrix}^T \tag{12b}$$

$$\mathbf{W}^a=\begin{bmatrix} w^a_{,1} & 0 & w^a_{,2}\\ 0 & w^a_{,2} & w^a_{,1}\end{bmatrix} \tag{12c}$$

$$\mathbf{w}^a=\begin{bmatrix} w^a_{,1} & w^a_{,2}\end{bmatrix}^T \tag{12d}$$

$$\mathbf{S}^a=\begin{bmatrix} \eta^a_{,1} & 0 & \eta^a_{,2}\\ 0 & \eta^a_{,2} & \eta^a_{,1}\end{bmatrix}^T \tag{12e}$$

$$\mathbf{s}^a=\begin{bmatrix} \eta^a_{,1} & \eta^a_{,2}\end{bmatrix} \tag{12f}$$

By collecting all nodal unknown fictitious values $\hat{p}^a(t)$ and $\hat{u}^a(t)$ into vectors $\hat{\mathbf{P}}$ and $\hat{\mathbf{U}}$, respectively, the system of the discretized equations (11) can be rewritten into matrix form, as follows:

$$\mathbf{M}\ddot{\hat{\mathbf{U}}}+\mathbf{K}\hat{\mathbf{U}}-\mathbf{Q}\hat{\mathbf{P}}=\mathbf{F} \tag{13a}$$

$$\mathbf{C}\dot{\hat{\mathbf{P}}}+\mathbf{H}\hat{\mathbf{P}}+\mathbf{G}\dot{\hat{\mathbf{U}}}=\mathbf{R} \tag{13b}$$

where $\mathbf{M}$ (mass matrix) and $\mathbf{C}$ (compressibility matrix) are evaluated taking into account the first integral term on the l.h.s. of equations (11a) and (11b), respectively; $\mathbf{K}$ (stiffness matrix) and $\mathbf{H}$ (permeability matrix) are computed considering the second term on the l.h.s. of equations (11a) and (11b), respectively; $\mathbf{Q}$ and $\mathbf{G}$ (coupling matrices) are calculated considering the third term on the l.h.s. of equations (11a) and (11b), respectively; and $\mathbf{F}$ and $\mathbf{R}$ (load nodal vectors) are evaluated considering the terms on the r.h.s. of equations (11a) and (11b), respectively.

It is important to note that equations (11) can be very easily implemented considering different spatial discretizations for each phase of the porous model; i.e., taking into account the present saturated porous media analysis, considering different discretizations for the solid and fluid sub-domains (e.g., different distribution and/or number of nodes, monomial basis with different orders, different weight functions etc.). This is highly important when null permeability is considered and incompressible fluid and solid particles are analysed, in order to provide unique solvability and convergence (see sub-section 4.2). Even when permeable and/or compressible models are focused, different phase discretizations allow more flexible and accurate analyses, characterizing the present methodology as a more efficient and robust numerical technique (local refinements can be considered independently for each phase, coupled systems of equations of lower order can be obtained etc.).

If different spatial discretizations for each phase are taken into account, the expressions for the matrices and vectors involved in equation (13) can be more generically written as:

$$\mathbf{M}_{ca} = \int_{\Omega^c} w_u^c \rho_m \eta_u^a d\Omega \tag{14a}$$

$$\mathbf{K}_{ca} = \int_{\Omega^c} \mathbf{W}_u^c \mathbf{D} \mathbf{S}_u^a d\Omega - \int_{\Gamma_u^c} w_u^c \mathbf{N} \mathbf{D} \mathbf{S}_u^a d\Gamma - \beta \int_{\Gamma_u^c} w_u^c \eta_u^a d\Gamma \tag{14b}$$

$$\mathbf{Q}_{ca} = \int_{\Omega^c} \mathbf{w}_u^c \alpha \eta_p^a d\Omega - \int_{\Gamma_u^c} w_u^c \mathbf{n} \alpha \eta_p^a d\Gamma \tag{14c}$$

$$\mathbf{C}_{ca} = \int_{\Omega^c} w_p^c (1/Q) \eta_p^a d\Omega \tag{14d}$$

$$\mathbf{H}_{ca} = \int_{\Omega^c} \mathbf{w}_p^{cT} \kappa \mathbf{s}_p^{aT} d\Omega - \int_{\Gamma_p^c} w_p^c \mathbf{n}^T \kappa \mathbf{s}_p^{aT} d\Gamma - \beta \int_{\Gamma_p^c} w_p^c \eta_p^a d\Gamma \tag{14e}$$

$$\mathbf{G}_{ca} = \int_{\Omega^c} w_p^c \alpha \mathbf{s}_u^a d\Omega \tag{14f}$$

$$\mathbf{F}_c = \int_{\Gamma_\tau^c} w_u^c \bar{\tau} d\Gamma + \int_{\Omega^c} w_u^c \rho_m \mathbf{b} d\Omega - \beta \int_{\Gamma_u^c} w_u^c \bar{\mathbf{u}} d\Gamma \tag{14g}$$

$$\mathbf{R}_c = \int_{\Gamma_q^c} w_p^c \kappa \bar{q} d\Gamma + \int_{\Omega^c} w_p^c a d\Omega - \beta \int_{\Gamma_u^c} w_p^c \bar{p} d\Gamma \tag{14h}$$

where subscripts u and p are relative to solid and fluid phase discretizations, respectively.

Once the ordinary differential matrix equations (13) are established, their coupled solution in the time-domain is discussed in the next sub-section, taking into account finite difference procedures.

3.3 Temporal discretization

For the temporal discretization, the following one-step finite difference approximations are considered (generalized Newmark method):

$$\ddot{\hat{\mathbf{U}}}^n = (1/(\gamma_2\Delta t^2))\,(\hat{\mathbf{U}}^n - \hat{\mathbf{U}}^{n-1}) - (1/(\gamma_2\Delta t))\dot{\hat{\mathbf{U}}}^{n-1} + (1 - 1/(2\gamma_2))\ddot{\hat{\mathbf{U}}}^{n-1} \tag{15a}$$

$$\dot{\hat{\mathbf{U}}}^n = (\gamma_1/(\gamma_2\Delta t))\,(\hat{\mathbf{U}}^n - \hat{\mathbf{U}}^{n-1}) + (1 - \gamma_1/\gamma_2)\dot{\hat{\mathbf{U}}}^{n-1} + \Delta t(1 - \gamma_1/(2\gamma_2))\ddot{\hat{\mathbf{U}}}^{n-1} \tag{15b}$$

$$\dot{\hat{\mathbf{P}}}^n = (1/(\gamma_3\Delta t))\,(\hat{\mathbf{P}}^n - \hat{\mathbf{P}}^{n-1}) + (1 - 1/\gamma_3)\dot{\hat{\mathbf{P}}}^{n-1} \tag{15c}$$

where Δt is the selected time-step and $\hat{\mathbf{U}}^n$ stands for a numerical approximation of $\hat{\mathbf{U}}(t_n)$. For an unconditionally stable scheme, the relations $\gamma_1 \geq 0.5$, $\gamma_2 \geq 0.5\,\gamma_1$ and $\gamma_3 \geq 0.5$ must hold in equations (15), whereγ_1, γ_2 and γ_3 are the parameters of the time integration method.

By introducing relations (15) into equations (13), the following final system of equations is obtained:

$$\begin{bmatrix} (1/(\gamma_2\Delta t^2))\mathbf{M} + \mathbf{K} & -\mathbf{Q} \\ (\gamma_1/(\gamma_2\Delta t))\mathbf{G} & (1/(\gamma_3\Delta t))\mathbf{C} + \mathbf{H} \end{bmatrix} \begin{bmatrix} \hat{\mathbf{U}}^n \\ \hat{\mathbf{P}}^n \end{bmatrix} = \begin{bmatrix} \bar{\mathbf{F}}^n \\ \bar{\mathbf{R}}^n \end{bmatrix} \tag{16}$$

where the r.h.s. of equation (16) is defined by:

$$\bar{\mathbf{F}}^n = \mathbf{F}^n + \mathbf{M}\,((1/(\gamma_2\Delta t^2))\hat{\mathbf{U}}^{n-1} + (1/(\gamma_2\Delta t))\dot{\hat{\mathbf{U}}}^{n-1} + (1/(2\gamma_2) - 1)\ddot{\hat{\mathbf{U}}}^{n-1}) \tag{17a}$$

$$\begin{aligned} \bar{\mathbf{R}}^n = \mathbf{R}^n + \mathbf{C}\,((1/(\gamma_3\Delta t))\hat{\mathbf{P}}^{n-1} + (1/\gamma_3 - 1)\mathbf{P}^{n-1}) + \\ + \mathbf{G}\,((\gamma_1/(\gamma_2\Delta t))\hat{\mathbf{U}}^{n-1} + (\gamma_1/\gamma_2 - 1)\dot{\hat{\mathbf{U}}}^{n-1} + \Delta t(\gamma_1/(2\gamma_2) - 1)\ddot{\hat{\mathbf{U}}}^{n-1}) \end{aligned} \tag{17b}$$

Solving the algebraic system of equations (16) at each time-step of the analysis enables the computation of the solid skeleton displacement and interstitial fluid pore-pressure time-histories.

4 Numerical aspects and applications

Two numerical applications are considered here, illustrating the discussed methodologies. In the first application, the simulation of a one-dimensional problem is focused, and a soil column is analysed taking into account different material properties. In the second application, a two-dimensional soil strip is considered. The results obtained by the proposed MLPG formulation are compared with analytical answers, whenever possible, and with results provided by the Finite Element Method (FEM).

In the present work, the radii of the influence domain and of the local sub-domain are set to $\theta_x d_i^3$ and $\theta_s d_i^1$, respectively; where d_i^3 and d_i^1 are the distances to the third and first nearest points from node i, respectively. In all the applications that follow, $\theta_x = 4.0$ and $\theta_s = 1.0$ are adopted. The time-integration parameters are selected regarding the trapezoidal rule, i.e.: $\gamma_1 = 0.5$, $\gamma_2 = 0.25$ and $\gamma_3 = 0.5$, and the mass and compressibility matrices are diagonalized by a row-sum technique.

4.1 Soil column

In this first example, a soil column is analysed (de Boer *et al.*, 1993; Diebels and Ehlers, 1996; Schanz and Cheng, 2000; Soares *et al.*, 2006; Soares, 2008). A sketch of the model is depicted in Fig.2. The top surface of the column is considered drained and uniformly loaded. The other surfaces of the model are undrained and have null normal displacements prescribed. 561 nodes are employed to spatially discretize the rectangular domain, in a regular equally spaced 33x17 (vertical and horizontal, respectively) distribution ($H = 10m$).

Two kinds of soils and load amplitudes are considered here (the loads have a Heaviside time variation). The properties of the models are specified below:

Model 1 (de Boer *et al.*, 1993; Diebels and Ehlers, 1996; Soares *et al.*, 2006; Soares, 2008) – for the present model, the load amplitude is 3 kN/m^2. The physical properties of the soil are: $\nu = 0.3$ (Poisson); $E = 14515880N/m^2$ (Young Modulus); $\rho_s = 2000kg/m^3$ (mass density – solid phase); $\rho_f = 1000kg/m^3$ (mass density – fluid phase); $\upsilon = 0.33$ (porosity); $\kappa = 10^{-6}m^4/Ns$ (permeability). The soil is incompressible and the time discretization considered is given by $\Delta t = 10^{-3}s$;

Model 2 (Schanz and Cheng, 2000; Soares *et al.*, 2006; Soares, 2008) – for the present model, the load amplitude is 1 kN/m^2. The physical properties of the soil are: $\nu = 0.298$; $E = 254423076.9N/m^2$; $\rho_s = 2700kg/m^3$; $\rho_f = 1000kg/m^3$; $\upsilon = 0.48$; $\kappa = 3.55 \cdot 10^{-9}m^4/Ns$. The soil is compressible and $K_s = 1.1 \cdot 10^{10}N/m^2$ (compression modulus – solid phase); $K_f = 3.3 \cdot 10^9 N/m^2$ (compression modulus – fluid phase). The time-step is $\Delta t = 10^{-4}s$.

In Fig.3, vertical displacements at point A are depicted, taking into account Model

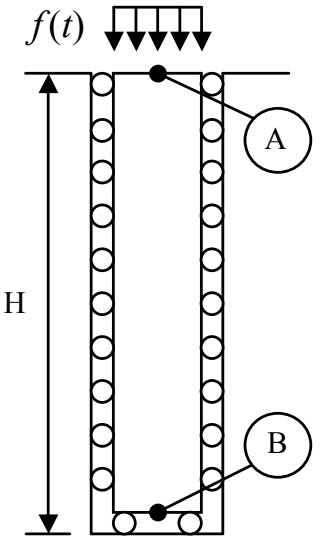

Figure 2: Sketch of the soil column model.

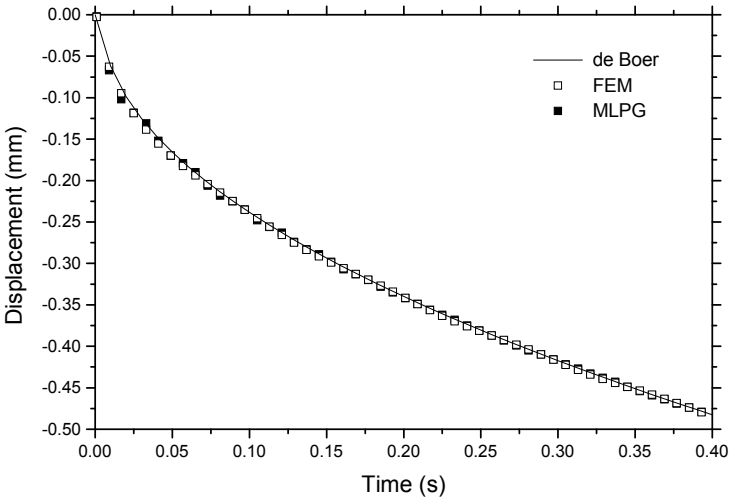

Figure 3: Displacements at point A for the incompressible soil column.

1. As can be observed, the results obtained by the MLPG formulation are in good agreement with the analytical results provided by de Boer *et al.* (1993) and with the results provided by the FEM. In Fig.4, vertical displacements at point A and pore-pressures at point B are presented, taking into account Model 2. Once again the MLPG results are in good agreement with the results provided by the semi-analytical procedures presented by Dubner and Abate (1968) and Schanz and Cheng (2000) and with those provided by the FEM.

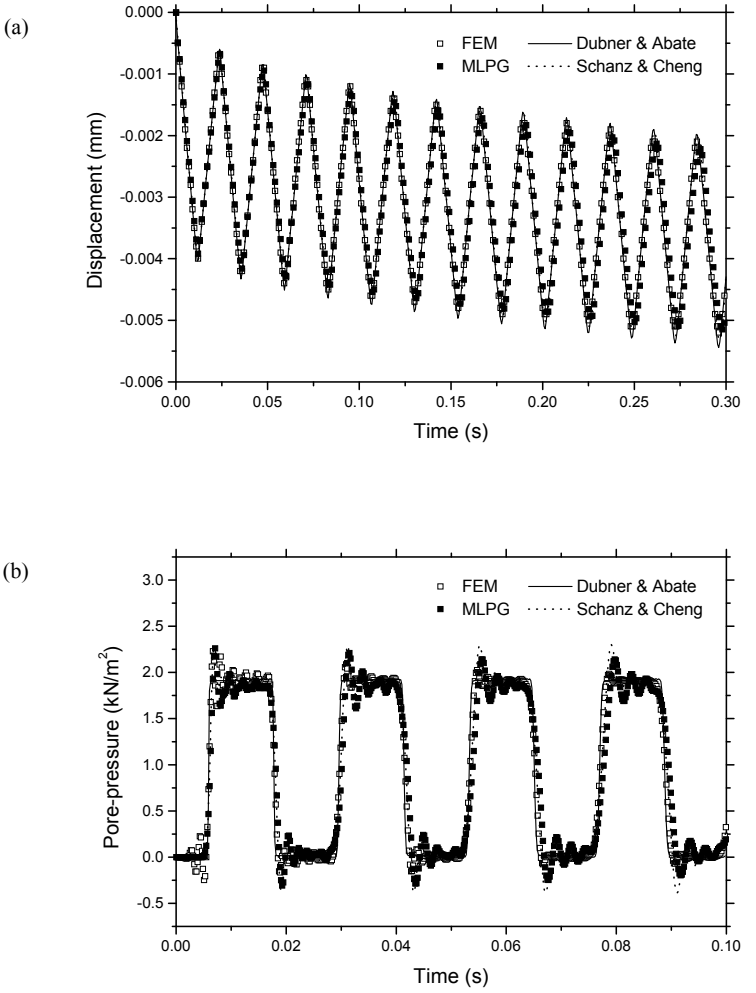

Figure 4: Compressible soil column: (a) displacements at point A; (b) pore-pressures at point B.

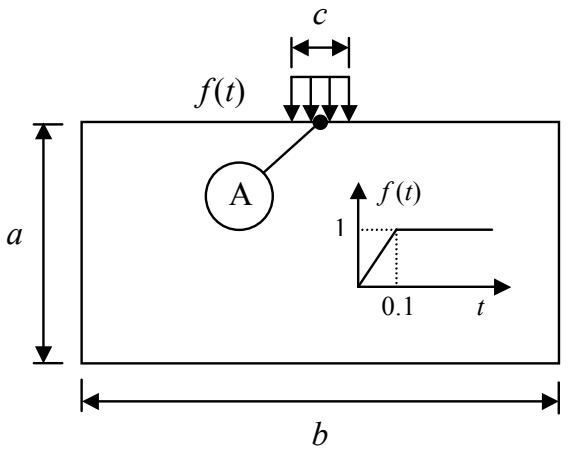

Figure 5: Sketch of the soil strip model.

4.2 Soil strip

In this second example, a two-dimensional soil strip is analysed (Li *et al.*, 2003; Soares *et al.*, 2006; Soares, 2008). A sketch of the model is depicted in Fig.5. The geometry of the strip is defined by $a = 5\,m$, $b = 10\,m$ and $c = 1\,m$. The symmetry of the model is taken into account and three possibilities are considered for the solid and fluid phase discretizations, namely:

Discretization 1 – 441 nodes are employed to spatially discretize the solid and the fluid phases, in a regular equally spaced 21x21 distribution, and complete monomial bases of order $m = 6$ (quadratic basis) are considered;

Discretization 2 – 441 nodes are employed to spatially discretize the solid and the fluid phases, in a regular equally spaced 21x21 distribution, and complete monomial bases of order $m = 6$ and $m = 3$ (quadratic and linear bases, respectively) are considered for the solid and fluid phases, respectively;

Discretization 3 – 441 nodes are employed to spatially discretize the solid phase, in a regular equally spaced 21x21 distribution, and 121 nodes are employed to spatially discretize the fluid phase, in a regular equally spaced 11x11 distribution. Complete monomial bases of order $m = 6$ are considered for both phases.

The soil strip is loaded as indicted in Fig.5 and the adopted time-step is $\Delta t = 5 \cdot 10^{-4} s$. Considering the physical properties of the medium, two models are focused here, namely:

Model 1 (Soares *et al.*, 2006; Soares, 2008) – the soil is compressible (fluid phase) and permeable: $\nu = 0.2$; $E = 10^7 N/m^2$; $\rho_s = 2538.5 kg/m^3$; $\rho_f = 1000 kg/m^3$;

$\upsilon = 0.35$; $\kappa = 10^{-7} m^4/Ns$ and $K_f = 3.3 \cdot 10^9 N/m^2$;

Model 2 (Li *et al.*, 2003; Soares, 2008) – same as Model 1, but the soil is impermeable and incompressible (i.e., $\kappa = 0$ and $K_s = K_f = \infty$).

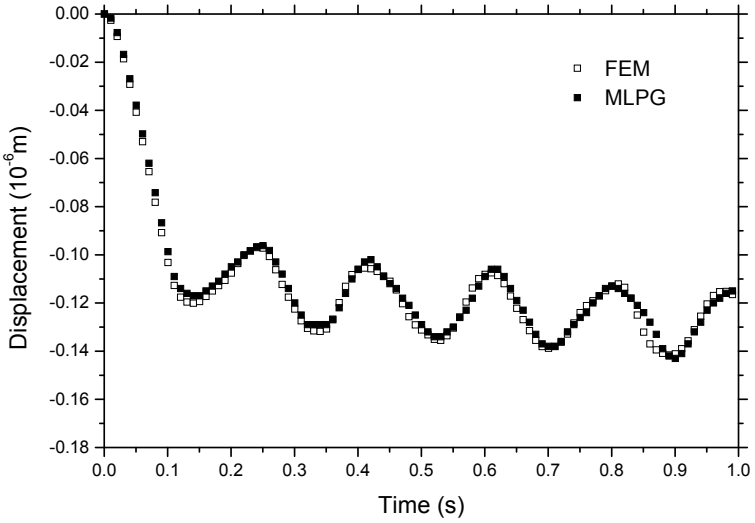

Figure 6: Displacements at point A for the soil strip considering Model 1 and Discretization 1.

Vertical displacements at point A (see Fig.5) are depicted in Fig.6, considering Discretization 1 and Model 1. As can be observed, the results provided by the proposed MLPG formulation are in good agreement with those provided by the FEM. In Fig.7, the pore-pressure distributions along the modelled soil strip are depicted, at time $t = 0.4s$, considering Model 1 and the three discretizations in focus. As can be observed, the three discretizations provide very similar results. As a matter of fact, Discretization 3 is a very appropriate discretization for the model (and for pore-mechanic analyses, in general): not only it renders a smaller system of coupled equations (providing more efficient analyses) than Discretizations 1 and 2, maintaining the good accuracy of the results, but also it allows the numerical simulation of impermeable and incompressible media, as is described in Fig.8.

Fig.8 depicts the pore-pressure distributions along the modelled soil strip at time $t = 1.0s$, considering Model 2 and the three discretizations in focus. As can be observed, Discretizations 1 and 2 do not fulfil the solvability condition, providing unstable results. On the other hand, Discretization 3 allows an appropriate numerical simulation of the model, and the results depicted in Fig.8(c) are in good agreement

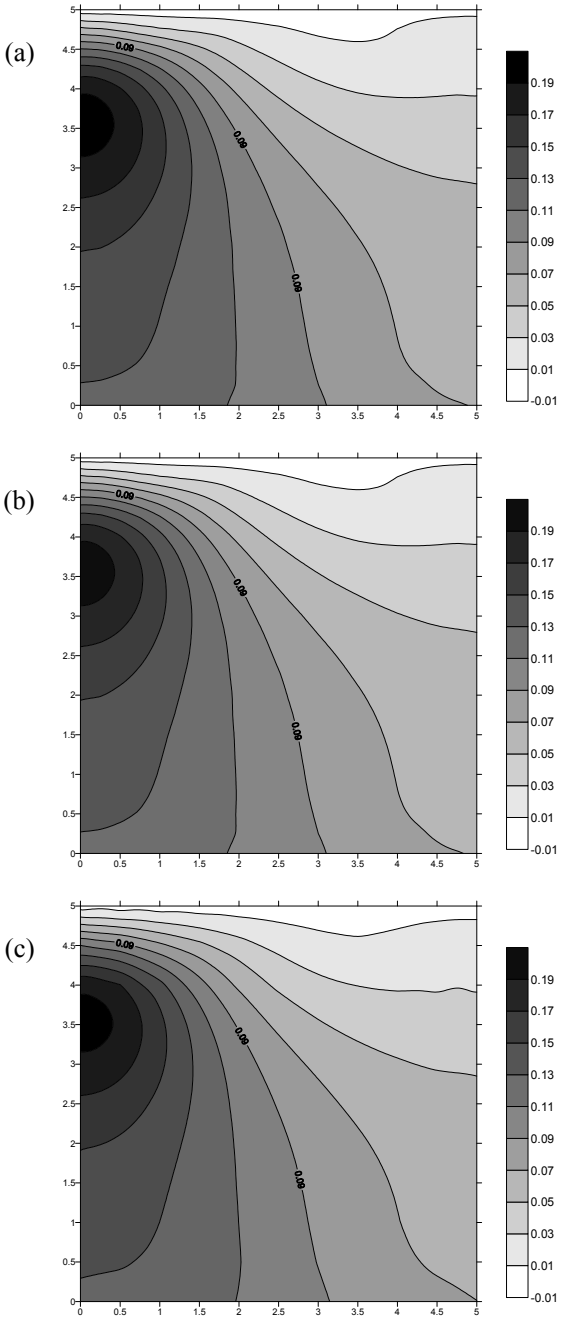

Figure 7: Pore-pressure field for the soil strip at time $t = 0.4s$ considering Model 1: (a) Discretization 1; (b) Discretization 2; (c) Discretization 3.

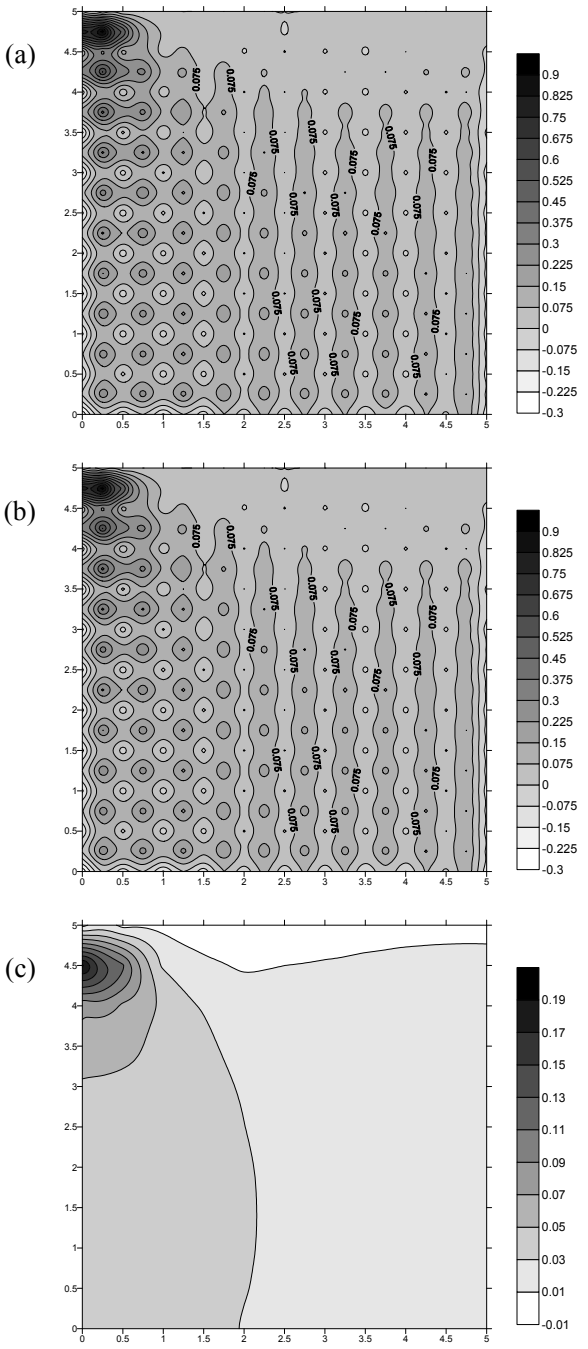

Figure 8: Pore-pressure field for the soil strip at time $t = 1.0s$ considering Model 2: (a) Discretization 1; (b) Discretization 2; (c) Discretization 3.

with other authors/methodologies results (see, for instance, Li *et al*., 2003).

Considering the present impermeable and incompressible model, the systems of equations (13), rewritten in a unified simplified form (see Belytschko *et al*., 2000, for an analogous procedure), read:

$$\begin{bmatrix} \mathbf{A}_{11} & \mathbf{A}_{12} \\ \mathbf{A}_{21} & \mathbf{0} \end{bmatrix} \begin{bmatrix} \mathbf{X}_1 \\ \mathbf{X}_2 \end{bmatrix} = \begin{bmatrix} \mathbf{B}_1 \\ \mathbf{0} \end{bmatrix} \tag{18}$$

where the conditions for solvability are (Bathe, 1996):

(i) $\mathbf{V}_1^T \mathbf{A}_{11} \mathbf{V}_1 > 0$ for all $\mathbf{V}_1$ satisfying $\mathbf{A}_{21} \mathbf{V}_1 = \mathbf{0}$;

(ii) $\mathbf{A}_{12} \mathbf{V}_2 = \mathbf{0}$ implies that $\mathbf{V}_2$ must be zero.

Thus, matrices $(\mathbf{A}_{21}^T \mathbf{A}_{21})$ and $(\mathbf{A}_{12}^T \mathbf{A}_{12})$ must be singular and nonsingular, respectively. If $n_2 > n_1$, this is not achieved and a necessary (but not sufficient) condition is that $n_1 \geq n_2$ (where n_1 and n_2 are the number of unknowns in vectors $\mathbf{X}_1$ and $\mathbf{X}_2$, respectively). When $n_1 > n_2$, matrix $(\mathbf{A}_{21}^T \mathbf{A}_{21})$ is always singular and this singularity is observed in the present application. Matrix $(\mathbf{A}_{12}^T \mathbf{A}_{12})$, on the other hand, must be carefully analysed. In the present application, for Discretizations 1 and 2, matrices $(\mathbf{A}_{12}^T \mathbf{A}_{12})$ are singular and, as a consequence, condition (ii) is not satisfied, implying in the spurious results depicted in Fig.8(a) and (b). On the other hand, for Discretization 3, conditions (i) and (ii) are fulfilled, and unique solvability is ensured, illustrating the importance of unequal phase discretization in the analysis of porous media.

5 Conclusions

In this work, time-domain dynamic analyses of porous media, taking into account MLPG formulations, are discussed. In the present MLPG formulation, Gaussian weight functions are adopted as test functions, eliminating boundary integrals along internal sub-domain contours, and a MLS interpolation scheme is considered, rendering a time-domain matricial system of coupled equations. The $\mathbf{u}-p$ formulation is focused and the coupled systems of equations that arise are characterized by incognita vectors whose entries are solid skeleton displacement and fluid interstitial pore-pressure fictitious nodal values. The expressions for the mass, compressibility, stiffness, permeability and coupling matrices, as well as for the load vectors, which define the system of equations governing the coupled model, taking into account different spatial discretizations for each phase, are presented along the text. This matricial system of coupled equations is analysed taking into account time-marching procedures based on the generalized Newmark method, which is an unconditionally stable time-marching technique, once appropriate time integration parameters are selected. Numerical results are presented at the end of the paper,

illustrating the good accuracy, stability and flexibility of the proposed methodologies.

The adoption of different spatial discretizations for each phase of the porous model is very important. Not only it may provide more accurate, efficient and flexible simulations, but also it permits the analysis of impermeable and incompressible media. It must be highlighted that the introduction of independent phase discretization by meshless local Petrov-Galerkin techniques is much easier to implement than in mesh-based formulations, such as the finite element method. In the present work a very generic methodology is discussed, allowing a complete independency of the solid and fluid phase discretizations (in fact, analyses can be carried out here without a single common node for both phases).

The framework presented in this paper is also very appropriate to analyse more complex physical models, as for instance, models governed by geometrical and/or material nonlinear formulations (see, for instance, Soares *et al*., 2010). In this case, meshless techniques may be considered very appropriate, not only to evaluate the current state of stresses properly (continuous variation of spatial derivatives of primary fields is obtained considering the present MLPG formulation), but also to avoid detrimental element distortions (usual in Lagrangian finite element approaches).

Acknowledgement: The financial support by CNPq (*Conselho Nacional de Desenvolvimento Científico e Tecnológico*) and FAPEMIG (*Fundação de Amparo à Pesquisa do Estado de Minas Gerais*) is greatly acknowledged.

References

Atluri, S.N. (2004): *The Meshless Method (MLPG) for Domain & BIE Discretizations*, Tech Science Press, Encino, CA.

Atluri, S.N., Shen, S. (2002): *The Meshless Local Petrov-Galerkin (MLPG) Method*, Tech Science Press, Encino,CA.

Atluri, S.N.; Shen, S.P. (2002): The meshless local Petrov-Galerkin (MLPG) method: A simple & less costly alternative to the finite element and boundary element methods, *CMES: Computer Modeling in Engineering & Sciences* vol.3, pp. 11-51.

Atluri, S.N.; Zhu, T. (1998): A New Meshless Local Petrov-Galerkin (MLPG) Approach in Computational Mechanics, *Computational Mechanics* vol.22, pp. 117-127.

Babuska, I. (1973): The finite element method with Lagrange multiplier, *Numerische Mathematik* vol.20, pp. 179-192.

Bathe, K.J. (1996): *Finite Element Procedures*, Prentice-Hall, Englewood Cliffs, New Jersey.

Belytschko, T., Liu, W.K., Moran, B. (2000): *Nonlinear Finite Elements for Continua and Structures*, Wiley, New York.

Bergamaschi, L. (2009): An Efficient Parallel MLPG Method for Poroelastic Models, *CMES: Computer Modeling in Engineering & Sciences* vol.29, pp. 191-215.

Biot, M.A. (1941): General theory of three-dimensional consolidation, *Journal of Applied Physics* vol.12, pp. 155–164.

Biot, M.A. (1956): The theory of propagation of elastic waves in a fluid-saturated porous solid. I. Low frequency range, *Journal of the Acoustical Society of America* vol.28, pp. 167–178.

Biot, M.A. (1956): The theory of propagation of elastic waves in a fluid-saturated porous solid. II. Higher frequency range, *Journal of the Acoustical Society of America* vol.28, pp. 179–191.

Biot, M.A. (1962): Mechanics of deformation and acoustic propagation in porous media, *Journal of Applied Physics* vol.33, pp. 1482–1498.

Brezzi, F. (1974): On the existence, uniqueness and approximation of saddle point problems arising from Lagragian multipliers, *RAIRO 8-R2*, pp. 129-151.

Chen, S.L., Li, Y.X. (2008): An efficient RPIM for simulating wave motions in saturated porous media. *International Journal of Solids and Structures* vol.45, pp. 6316-6332.

de Boer, R. (1998): *Theory of porous media – highlights in the historical development and current state*, Springer, Berlin.

de Boer, R., Ehlers, W., Liu, Z. (1993): One-dimensional transient wave propagation in fluid saturated incompressible porous media, *Archive of Applied Mechanics* vol.63, pp. 59-72.

Diebels, S., Ehlers, W. (1996): Dynamic analysis of a fully saturated porous medium accounting for geometrical and material non-linearities. *International Journal for Numerical Methods in Engineering* vol.49, pp. 833-848.

Dubner, H., Abate, J. (1968): Numerical inversion of Laplace transforms by relating them to the finite Fourier cosine transform, *Journal of the Association for Computing Machinery* vol.15, pp. 115-123.

Ehlers, W., Bluhm J. (eds) (1998): *Porous media – theory, experiments and numerical applications*, Springer, Berlin.

Ferronato, M., Mazzia, A., Pini, G., Gambolati, G. (2007): A meshless method

for axi-symmetric poroelastic simulations: Numerical study, *International Journal for Numerical Methods in Engineering* vol.70, pp. 1346-1365.

Huang, M.S., Yue, Z.Q., Tham, L.G., Zienkiewicz, O.C. (2004): On the stable finite element procedures for dynamic problems of saturated porous media, *International Journal for Numerical Methods in Engineering* vol.61, pp. 1421-1450.

Huang, M.S., Zienkiewicz, O.C. (1998): New unconditionally stable staggered solution procedures for coupled soil-pore fluid dynamic problems, *International Journal for Numerical Methods in Engineering* vol.43, pp. 1029-1052.

Karim, M.R. Nogami, T. Wang, J.G. (2002): Analysis of transient response of saturated porous elastic soil under cyclic loading using element-free Galerkin method, *International Journal of Solids and Structures* vol.39, pp. 6011-6033.

Lewis, R.W., Schrefler, B.A. (1998): *The finite element method in the static and dynamic deformation and consolidation of porous media* (2^{nd} ed), John Wiley & Sons, Chichester.

Li, X., Han, X., Pastor, M. (2003): An iterative stabilized fractional step algorithm for finite element analysis in saturated soil dynamics, *Computational Methods in Applied Mechanics and Engineering* vol.192, pp. 3845-3859.

Lin, H.; Atluri, S.N. (2000): Meshless local Petrov-Galerkin (MLPG) method for convection-diffusion problems, *CMES: Computer Modeling in Engineering & Sciences*, vol.1, pp. 45-60.

Modaressi, H., Aubert, P. (1998): Element-free Galerkin method for deforming multiphase porous media, *International Journal for Numerical Methods in Engineering* vol.42, pp. 313-340.

Murakami, A., Setsuyasu, T., Arimoto, S. (2005): Mesh-free method for soil-water coupled problem within finite strain and its numerical validity, *Soils and Foundations* vol.45, pp. 145-154.

Nogami, T., Wang, W., Wang, J.G. (2004): Numerical method for consolidation analysis of lumpy clay fillings with meshless method, *Soils and Foundations* vol.44, pp. 125-142.

Oliaei, M.N. (2009): Some numerical issues using element-free Galerkin meshless method for coupled hydro-mechanical problems, *International Journal for Numerical and Analytical Methods in Geomechanics* vol.33, pp. 915-938.

Pastor, M., Li, T., Liu, X., Zienkiewicz, O.C. (1999): Stabilized low-order finite elements for failure and localization problems in undrained soils and foundations, *Computational Methods in Applied Mechanics and Engineering* vol.174, pp. 219-234.

Pastor, M., Li, T., Liu, X., Zienkiewicz, O.C., Quecedo, M. (2000): A frac-

tional step algorithm allowing equal order of interpolation for coupled analysis of saturated soil problems, *Mechanics of Cohesive-Frictional Materials* vol.5, pp. 511-534.

Schanz, M., Cheng, A.H.D. (2000): Transient wave propagation in a one-dimensional poroelastic column, *Acta Mechanica* vol.145, pp. 1-18.

Sladek, J.; Sladek, V.; Zhang, C.Z. (2003): Application of meshless local Petrov-Galerkin (MLPG) method to elastodynamic problems in continuously nonhomogeneous solids, *CMES: Computer Modeling in Engineering & Sciences* vol.4, pp. 637-647.

Sladek, J.; Sladek, V.; Zhang, C.Z.; Tan C.L. (2006): Meshless local Petrov-Galerkin Method for linear coupled thermoelastic analysis, *CMES: Computer Modeling in Engineering & Sciences* vol.16, pp. 57-68.

Soares Jr., D. (2008): A time-domain FEM approach based on implicit Green's functions for the dynamic analysis of porous media, *Computational Methods in Applied Mechanics and Engineering* vol.197, pp. 4645–4652.

Soares Jr., D., Sladek, J., Sladek, V. (2010): Nonlinear dynamic analyses by meshless local Petrov-Galerkin formulations, *International Journal for Numerical Methods in Engineering* vol.81, pp. 1687–1699.

Soares Jr., D., Telles, J.C.F., Mansur, W.J. (2006): A time-domain boundary element formulation for the dynamic analysis of non-linear porous media, *Engineering Analysis with Boundary Elements* vol.30, pp. 363-370.

Wang, J.G., Karim, M.R., Lin, P.Z. (2007): Analysis of seabed instability using element free Galerkin method, *Ocean Engineering* vol.34, pp. 247-260.

Wang, J.G., Liu, G.R., Lin, P. (2002): Numerical analysis of Biot's consolidation process by radial point interpolation method, *International Journal of Solids and Structures* vol.39, pp. 1557-1573.

Wang, J.G., Xie, H., Leung, C.F. (2009): A local boundary integral-based meshless method for Biot's consolidation problem, *Engineering Analysis with Boundary Elements* vol.33, pp. 35-42.

Wang, J.G., Yan, L., Liu, G.R. (2005): A local radial point interpolation method for dissipation process of excess pore water pressure, *International Journal of Numerical Methods for Heat & Fluid Flow* vol.15, pp. 567–587.

Wang, J.G., Zhang, B.Y., Nogami, T. (2004): Wave-induced seabed response analysis by radial point interpolation meshless method, *Ocean Engineering* vol.31, pp. 21-42.

Wang, W.D., Wang, J.G., Wang, Z.L., Nogami, T. (2007): An unequal-order radial interpolation meshless method for Biot's consolidation theory, *Computers*

and Geotechnics vol.34, pp. 61-70.

Wang, Z.L., Li, Y.C. (2006): Analysis of factors influencing the solution of the consolidation problem by using an element-free Galerkin method, *Computers & Geosciences* vol.32, pp. 624-631.

Wang, Z.L., Wang, J.G., Shen, R.F. (2008): The application of a meshless method to consolidation analysis of saturated soils with anisotropic damage, *Computers & Geosciences* vol.34, pp. 849-859.

Zienkiewicz, O.C., Chan, A.H.C., Pastor, M., Paul, D.K., Shiomi, T (1990): Static and dynamic behavior of soils: a rational approach to quantitative solutions. I. Fully saturated problems, *Proceedings of the Royal Society of London* vol.429, pp. 285-309.

Zienkiewicz, O.C., Chan, A.H.C., Pastor, M., Schrefler, B.A., Shiomi, T. (1999): *Computational geomechanics with special reference to earthquake engineering*, John Wiley & Sons, Chichester.

Zienkiewicz, O.C., Qu, S., Taylor, R.L., Nakzawa, S. (1986): The patch test for mixed formulation, *International Journal for Numerical Methods in Engineering* vol.23, pp. 1871-1883.

Zienkiewicz, O.C., Shiomi, T. (1984): Dynamic behavior of saturated porous media: the generalized Biot formulation and its numerical solution, *International Journal for Numerical and Analytical Methods in Geomechanics* vol.8, pp. 71-96.